Phonon wave-packet simulations of Ar/Kr interfaces for thermal rectification

N. A. Roberts and D. G. Walker[a)]
Department of Mechanical Engineering, Vanderbilt University, Nashville, Tennessee 37235, USA

(Received 1 July 2010; accepted 20 October 2010; published online 23 December 2010)

The frequency and direction dependence of transmission coefficients at interfaces was investigated theoretically. The interfaces are formed by having two Lennard-Jones materials differing in mass and interatomic potential equally divided at the center of an fcc lattice system. A single frequency wave-packet is generated at one end of the system and allowed to propagate through the system until all interactions with the interface are complete. The transmission coefficient is then calculated by comparing the energy of the packet that is transmitted with the original wave-packet. Results show a difference in transmission when the wave-packet originates from opposite sides. © *2010 American Institute of Physics*. [doi:10.1063/1.3517159]

I. INTRODUCTION

Thermal rectification is a phenomenon where the magnitude of transport in a specific direction through a material is dependent on the sign of the temperature gradient, and though observations of the effect in solids have been rare, rectifying behavior could have widespread applications. Materials with different thermal transport properties in opposite directions along the same axis would revolutionize how thermal management problems from the nanoscale and microscale to the macroscale are approached. Thermal management has been an issue and is becoming even more important in microelectronics where device sizes are becoming smaller,[1] increased chip densities, increasing importance of interconnects,[2] and emerging technologies such as three-dimensional circuit designs[3] make heat removal extremely difficult. Materials that exhibit thermal rectification would drastically improve our ability to control the flow of heat in microelectronic devices similar to the way we are able to control the flow of charge carriers. These materials would also greatly aid in the design of thermoelectric devices by designing them to have extremely low thermal conductivities in the one direction.[4] Thermally rectifying materials would allow engineers to design chips that preferred transport along a specific direction (e.g., to a location to dissipate heat) while providing resistance to the flow of heat toward temperature sensitive portions of the chip (logic circuits). Clearly, this would allow for more compact and higher performance circuits.

Records of thermal rectification date back as early as 1935 when Starr[5] found that copper-cuprous oxide systems showed thermal as well as electrical rectification. Since this original observation there have been several reports of thermal rectification in systems with a contact between similar and dissimilar materials which have shown thermal rectifying behavior. In 2002, Terraneo *et al.*[6] demonstrated theoretical rectification behavior using a nonlinear one-dimensional chain of atoms between two thermostats at different temperatures. In their system, Terraneo was able to change the chain from a normal conductor in one direction to a nearly perfect insulator in the other direction due to the nonlinearity of the potential. Since this study several studies have shown improvements over this rectifier.[7–9] In 2006, Walker[10] reviewed several candidate theoretical models based on geometric asymmetries with unequal thermal expansion and offered several alternate explanations for rectification behavior based on nonequilibrium effects. Examples of these models include lattice vibrations which reflect differently depending on the geometry and characteristics of the structure or transmission across an interface. Since this work was conducted there have been several studies that model nanostructured materials and show promising results for thermal rectifiers. All of these materials include some asymmetry either geometrically or from material composition.[11–14] There has also been one experimental study of nonuniformly mass loaded nanotubes composed of carbon and boron nitride which showed up to a 7% greater transport in the direction of decreasing mass density.[15]

In addition to the theoretical studies of nanomaterials with asymmetries, interfaces have also been proposed as rectifying structures. Recently, there have been theoretical studies that show asymmetric phonon transport in nanostructured interfaces.[16,17] These studies have shown a preferred transport direction across the interface, but a detailed understanding of phonon transport at interfaces is lacking. Models for the prediction of thermal boundary conductance at interfaces have been around since the 1950s,[18] but they do not include a directional dependence on the transport. At perfect planar interfaces between dissimilar materials we expect minimum phonon scattering to occur which means if the materials composing the interface have large differences in frequency content we would expect the transmission probability to be greater in one direction over another based on the difference in the phonon dispersion of the materials. In this work, we will investigate the direction and frequency dependence of the phonon transmission probability at an interface between dissimilar materials. To perform this study, we use a molecular dynamics package to perform phonon wave-packet simu-

a)Electronic mail: greg.walker@vanderbilt.edu.

lations by creating and following a single frequency wave in the system and allowing it to interact with the interface.[19–22] The results show asymmetric phonon transmission in perfect planar and varying levels of diffuse interfaces in which atoms of each material type exist on both sides of the interface.

II. SIMULATION METHOD

Large-scale atomic/molecular massively parallel simulator (LAMMPS), a general purpose molecular dynamics package developed at Sandia National Laboratory,[23] is used to perform phonon wave-packet simulations in an argon/krypton system. The argon and krypton in the system use Lennard-Jones (L-J) potential parameters from the literature.[24] The transmission coefficients are determined for a range of frequencies from argon to krypton and the reverse. The transmission coefficients are obtained by generating a wave-packet given by[19]

$$u_n = A\epsilon \exp[ik(z_n - z_o)^2]\exp[-(z_n - z_o)^2/\xi^2], \quad (1)$$

where A is the amplitude of the displacement, ϵ is the polarization vector, k is the wave vector, z_n is the location of the atom along the direction of transport, z_o is the center of the wave-packet, and ξ is the width of the wave-packet. In all the simulations $A=0.002a$, $\epsilon=1$, $z_o=250a$, k ranges from $0.1\times(2\pi/a)$ to $0.9\times(2\pi/a)$, and $\xi=100a$ where a is the lattice constant of the material in which the wave-packet is generated. All wave-packets in this work were transverse acoustic packets, therefore we are assuming only a single dispersion branch instead of a full dispersion. The system we simulate is $1000a\times 2a\times 2a$ ($500a$ argon and $500a$ krypton, which results in greater than half of the length being krypton because $a_{Kr} > a_{Ar}$) so that it is long enough to create a large enough wave packet ($100a$ in length) far enough away from the interface so that it is able to propagate, interact and move away from the interface in order to collect information on the energy transmitted and reflected during the interaction. All boundaries in this system (x,y,z) are periodic. The wave-packet and system must also satisfy $l > \xi > \lambda$ where l is the phonon mean free path and λ is the wavelength.[22]

The simulations are run at 0° so that only the prescribed phonon wave-packet exists in the lattice. The transmission coefficient is calculated by taking the ratio of the energy of the transmitted and incident wave-packets given by[22]

$$\mathcal{T} = \left(\frac{E_{tr}}{E}\right), \quad (2)$$

where E_{tr} is the transmitted energy and E is the original wave-packet energy. An additional simulation was run with no displacement and was used as the base energy for the total, argon and krypton portions of the system. This base energy was subtracted from the simulations with wave-packets. The initial wave-packet energy was the initial potential energy added by the displacements and the transmitted energy was the added energy in the other material once the wave-packet interacted and moved away from the interface.

Validation of the simulation was performed by initializing a wave-packet in a device composed of a single material (argon in this case). The full range of wave vectors were simulated and the result was perfect transmission of the wave-packet along the device.

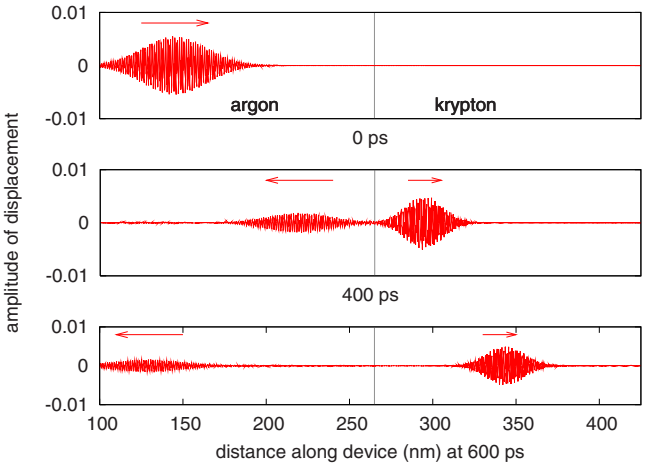

FIG. 1. (Color online) Wave-packet propagation originating in the argon with a normalized wave vector of 0.4. The view does not include the entire simulation domain.

III. SIMULATION RESULT

In this work the wave-packet was generated in the argon side of the interface and was monitored as it propagated and interacted with the interface. This interaction with the interfaces resulted in some transmission into the krypton and some reflection back into the argon. In the next step, the wave-packet was generated in the krypton and allowed to propagate and interact with the interface. Again in this second case some of the wave-packet transmitted into the argon while some was reflected back into the krypton. Figure 1 shows the propagation of a wave-packet originating in argon with a wave vector of $k=0.4\times(2\pi/a)$ near the interface. Figure 2 shows the propagation of a wave-packet originating in the krypton with the same wave vector as in Fig. 1. In Fig. 2, some additional waves are seen because of the periodicity of the simulation domain and the higher phonon velocity in

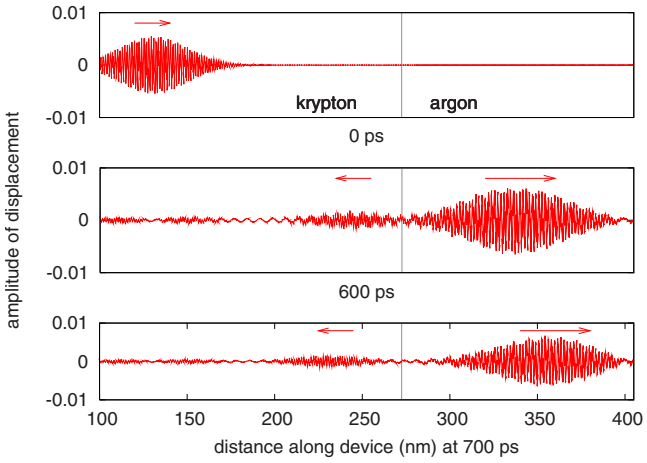

FIG. 2. (Color online) Wave-packet propagation originating in the krypton with a normalized wave vector of 0.4. Some additional waves are seen in the 600 and 700 ps frame due to the periodic boundary conditions used in the simulation. The view does not include the entire simulation domain.

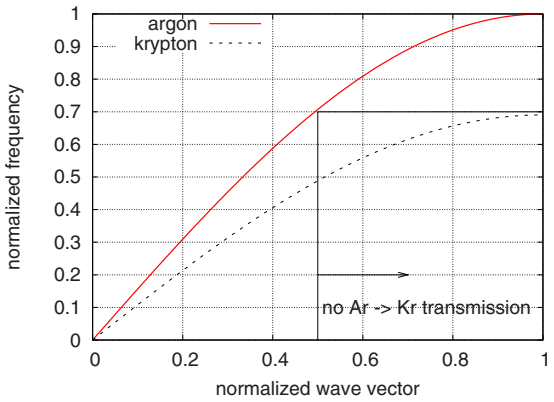

FIG. 3. (Color online) Comparison of a single branch of an analytic dispersion for argon and kryptonlike materials.

the argon. These observed wave-packets do not affect the calculated transmission coefficients because they have only interacted with a single interface at the time the energies are computed. By comparing these two figures we see that the transmission probabilities are similar, but the wavelength of the wave-packets are different because of energy conservation. Since the energy/frequency of the phonon must be the same there must be a change in the phonon wavelength because of the difference in phonon dispersion between the two materials because of the difference in mass and potential parameters. An analytic dispersion of each of the materials is shown in Fig. 3 where a difference is seen between argon and krypton. From the dispersion of the two materials we expect that a wave-packet originating in the argon with a wave vector greater than about $0.5\times(2\pi/a)$ would be completely reflected because there are no transverse acoustic phonons at frequencies that large in krypton.

The transmission coefficients calculated for both the wave-packet originating in the argon and the wave-packet originating in the krypton are shown in Fig. 4. The error in the data was a result of numerical fluctuations in the simulation. The acoustic mismatch model (AMM)

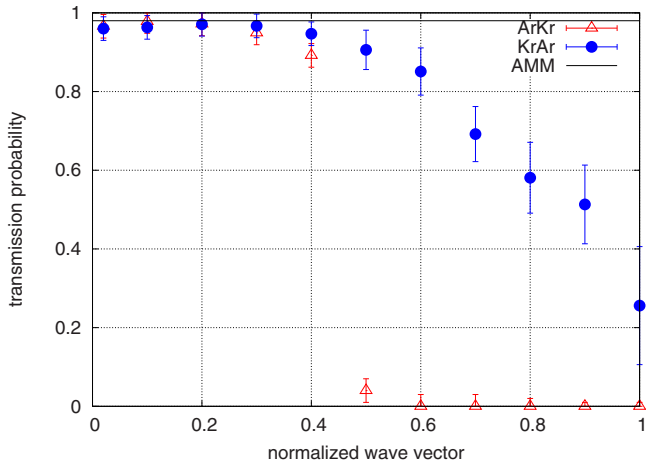

FIG. 4. (Color online) Transmission coefficients of wave-packets propagating from argon and krypton into the opposite as a function of wave vector.

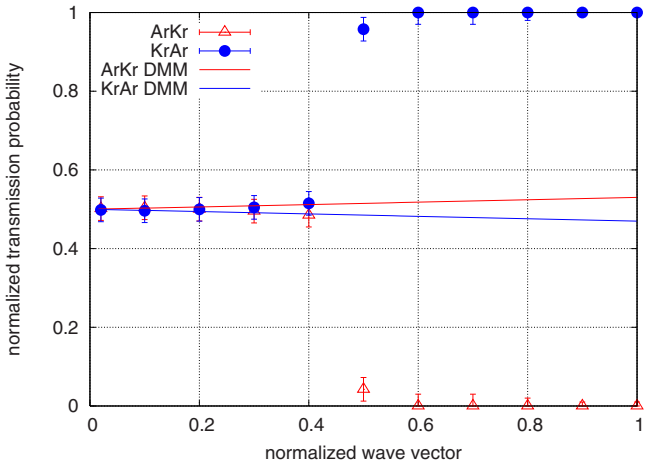

FIG. 5. (Color online) Normalized transmission coefficients of wave-packets propagating from argon and krypton into the opposite as a function of wave vector with the prediction from the DMM.

$$\mathcal{T}_{\mathrm{AMM}}=\frac{4Z_{\mathrm{Ar}}Z_{\mathrm{Kr}}}{(Z_{\mathrm{Ar}}+Z_{\mathrm{Kr}})^2}, \tag{3}$$

is a model used for the calculation of transmission probabilities where Z_{Ar} and Z_{Kr} are the acoustic impedances of the argon and krypton, respectively. The AMM assumes that phonons are governed by continuum acoustics and that phonons can only reflect, reflect and mode convert, refract or refract and mode convert.[18] This model does not include any directional dependence and is based on the impedance of the two materials creating the interface. The diffuse mismatch model (DMM) is given by

$$\mathcal{T}_{\mathrm{DMM},i}(\omega)=\frac{V_{g,i+1}(\omega)N_{i+1}(\omega,T)}{V_{g,i}(\omega)N_i(\omega,T)+V_{g,i+1}(\omega)N_{i+1}(\omega,T)}, \tag{4}$$

where V_g is the phonon group velocity and N is the phonon occupation number. The DMM assumes that when a phonon interacts with an interface it loses all memory of where it originated and the phonon selects which material it transmits into based on the probability calculated. A formulation is needed here to account for the probability that a phonon originated from a specific side (either the argon or krypton) in order to calculate the transmission from one material into the other. In Fig. 5, the transmission probabilities have been combined assuming phonons are propagating from both ends of the device and the transmission probability in each direction is the transmission in the specified direction divided by the sum of the transmission in both directions or

$$\bar{\mathcal{T}}_A=\frac{\mathcal{T}_A}{\mathcal{T}_A+\mathcal{T}_B}. \tag{5}$$

This is the form of the transmission that is obtained from the DMM which gives some directional dependence based on the ratio of density of states and phonon group velocities. The DMM predictions for the argon/krypton system are included in Fig. 5. Clearly the DMM does not match the results from the wave-packet simulations and this is because the DMM does not consider the phonon dispersion in the calculation of the transmission probability. If argon and krypton both had similar dispersions in that the maximum frequency

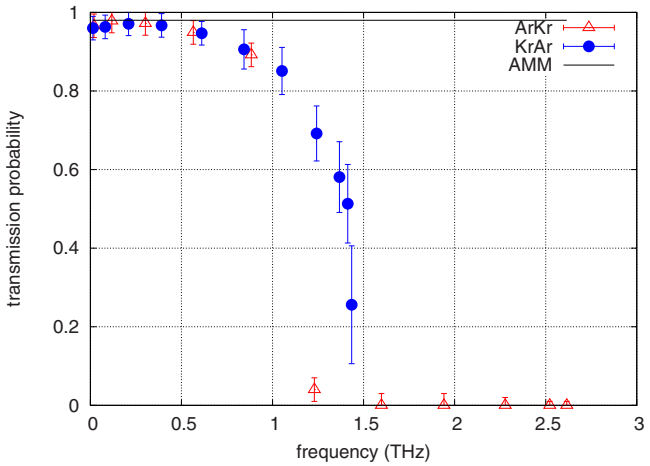

FIG. 6. (Color online) Transmission coefficients of wave-packets propagating from argon and krypton into the opposite as a function of frequency.

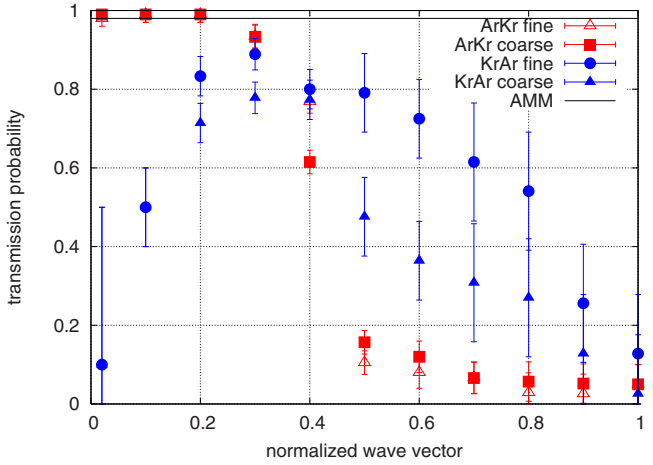

FIG. 7. (Color online) Transmission coefficients of wave-packets propagating from argon and krypton into the opposite as a function of normalized wave vector in diffuse interfaces.

of each is commensurate, we would expect the wave-packet results to match the DMMs trend to some extent. Because they are finite and the maximum frequency of this branch in krypton is well below that of argon, the trends are far from expected from the DMM. From the phonon wave-packet simulations at low wave vectors the transmission from the argon to the krypton is greater and is close to the prediction from the AMM as expected.[18] At higher wave vectors the transmission is greater from the krypton to the argon and diverges from the AMM, but does not match the DMM. The transmission coefficient from the argon to the krypton becomes zero at a wave vector greater than 0.5. No transmission is expected in this case because there are no frequency modes in the krypton at this particular frequency (see Fig. 3). Our expectation that no transmission should occur is based on the difference in phonon dispersion and the assumption that there is no inelastic scattering at the interface.[21] Since the DMM calculation only considers the frequency dependence of the group velocity and the ratio of density of states and not the dispersion there is a calculated probability of transmission even when those phonon frequencies are not possible when no inelastic scattering occurs. A system at 0° and having a perfect planar interface should exhibit no inelastic scattering and therefore perfect reflection. These results show that there is indeed a wave vector dependence on the phonon transmission at the interface between dissimilar materials. A dependence on wave vector is not necessarily of importance here since we are interested in energy transport across an interface. Figure 6 shows the phonon transmission coefficient as a function of phonon frequency. We obtained the frequency and the group velocity of the wave-packet for the specific wave vector from the molecular dynamics simulations which agreed well with the analytic dispersion and the literature for argon and krypton.[25–27] The transmission as a function of frequency appears to be slightly different around the maximum frequency in the krypton where no inelastic scattering occurs. This difference in transmission at this small frequency range could possible be exploited to produce thermal rectification. To determine the extent, thermal conductance calculations were performed, and the results are provided at the end of this section.

Diffuse interfaces were also examined in this work. Figure 7 shows the transmission as a function of the normalized wave vector for the diffuse interface cases with a varying level of diffusion. The diffusion at the interface results in a redistribution of phonon energies, where a high frequency phonon can be scattered into multiple lower frequency phonons. This multiphonon scattering is seen when a phonon in the argon of a frequency greater than the maximum frequency of the krypton is partially transmitted. This effect known as inelastic scattering is a results of strain from the different materials at the interface. This effect is increased with the diffusing of atoms at the interface which effectively increase the region of increased strain. This effect from the strain is an anharmonic effect that is usually attributed to temperature. Transmission of a phonon at the higher frequency could only occur if the phonon was either inelastically scattered or converted to another phonon branch. In this work, we are not able to distinguish the difference. The transmission above the maximum frequency of krypton increases from argon to krypton as the level of diffusion at the interface increases while the transmission below the maximum frequency of krypton decreases for all cases. This is a result of increased scattering at the interface which would decrease the transmission of allowed frequencies and increase the transmission of frequencies that are not allowed. Figure 8 shows the transmission coefficients as a function of the phonon frequency for each of the diffuse interfaces. It is clear from this figure that the diffusion at the interface acts to scatter phonons. In the frequency range that is present in both materials we see a reduction in the transmission probabilities due to diffuse scattering at the interface. In the frequency range above the maximum frequency in krypton we see that the probability of phonon transmission from the argon into the krypton increases, which was also observed by Zhao and Freund.[28] This increase in phonon transmission probability in this region is due to inelastic scattering due to the increased potential energy from strain at the interface. As the region of the diffuse interface is increased we see that the transmission probabilities also increased due to increased inelastic scattering. For verification, we look at the potential

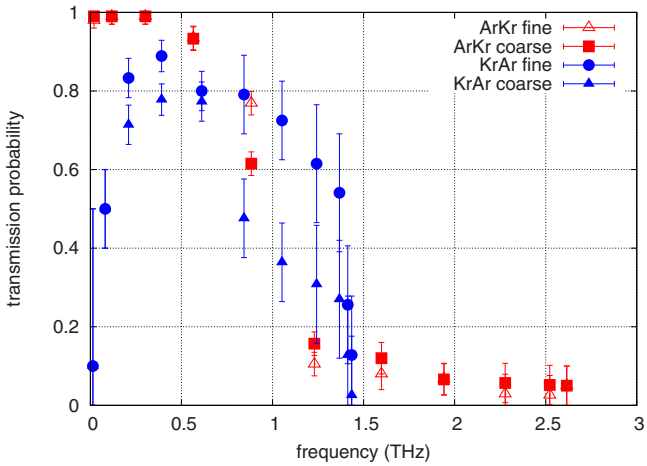

FIG. 8. (Color online) Transmission coefficients of wave-packets propagating from argon and krypton into the opposite as a function of frequency in diffuse interfaces.

energy of the system before the wave-packet is added to determine the amount of potential energy due to strain in each of the interfaces. Note that this energy is also the total energy of the system because the amount of kinetic energy is negligible small. This potential energy has a similar effect as temperature by making the motion of the atoms anharmonic. Table I shows the initial potential energy of each of the systems where the difference is due to the amount diffusion at the interface. The perfect interface is a single planar interface, the fine interface has a one unit cell diffusion region and the coarse has a five unit cell diffusion region was created using an error function weighted at 50% and a decay constant of the specified diffusion region. These diffusion regions are created using a random number and comparing it to the value of the error function. If the random number is less than the value of the error function the atom is switched with an atom of the other material on the opposite side of the interface. The values of the potential energy shown here are negative because the energy between atoms in lattice fall in the negative section of the potential function shown in Fig. 9. In the case of no potential energy due to strain, the atoms will sit at the minimum of the potential well and the system will have a minimized energy. In the case of the diffuse interfaces, the atoms in the interface region will be away from the minimum energy position along the side of the potential well which is what occurs at higher temperatures (greater thermal energy).

To investigate these interfaces as thermal rectifiers or how the asymmetry in phonon transmission coefficients can result in thermal rectification, we compute the heat flux from each side of the device using a Landauer-Buttiker formalism[29]

TABLE I. Potential energy of each system for the different interfaces.

Interface	Potential energy (eV)
Perfect	−1566.9429
Fine diffuse	−1559.0857
Coarse diffuse	−1559.0035

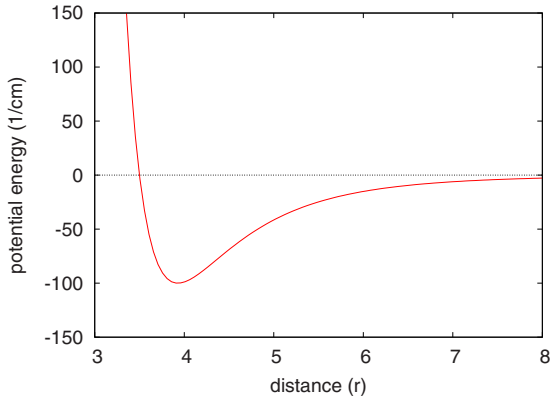

FIG. 9. (Color online) Example potential function from the 12–6 L-J potential.

$$q_{1-2} = \int_0^{\omega_{1,\max}} \hbar\omega_1' D_1(\omega_1') n(\omega_1', T_1) \mathcal{T}_1(\omega_1') v_1(\omega_1') d\omega_1', \quad (6)$$

$$q_{2-1} = \int_0^{\omega_{2,\max}} \hbar\omega_2' D_2(\omega_2') n(\omega_2', T_2) \mathcal{T}_2(\omega_2') v_2(\omega_2') d\omega_2', \quad (7)$$

where $D(\omega)$ is the phonon density of states, $n(\omega, T)$ is the Bose–Einstein distribution, $\mathcal{T}(\omega)$ is the phonon transmission coefficient calculated from the wave-packet simulations, and $v(\omega)$ is the phonon velocity. Numerical integration using the trapezoidal rule was used for the calculation because of the discrete nature of our data. Although actual heat flux calculations should include all modes and polarizations, we have involved the transmission of the transverse acoustic branch only. Realize, that the mechanisms identified from the results are not specific to TA phonons. Moreover, TA phonons are the primary energy carriers in this system. Therefore, we expect rectification to manifest itself in a system where all modes are considered simultaneously. The total heat flux (shown in Fig. 10) is computed from the sum of heat fluxes in each direction.

$$q^+ = q_{1-2} - q_{2-1}, \quad T_1 > T_2, \quad (8)$$

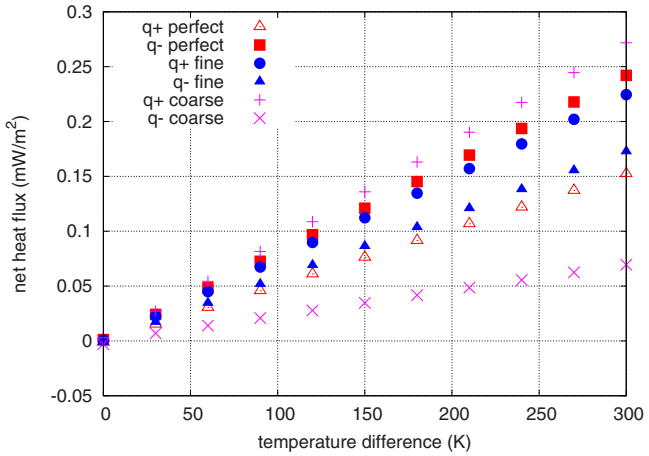

FIG. 10. (Color online) Net flux in the positive and negative directions calculated based on Eq. (9) with the transmission coefficients calculated from molecular dynamics simulations.

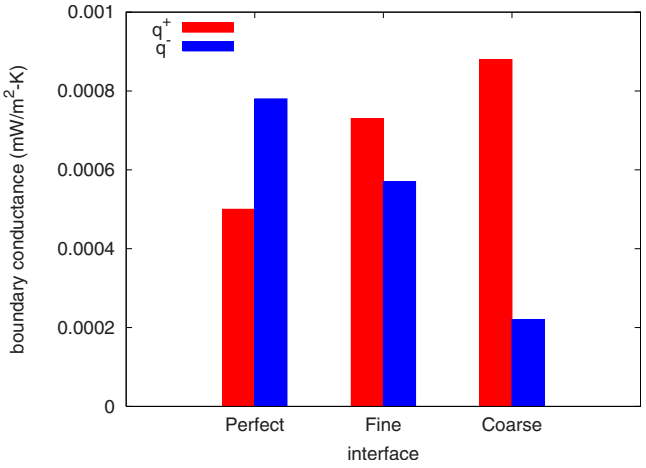

FIG. 11. (Color online) Conductance in the forward and reverse directions for the various interface conditions.

$$q^- = q_{2-1} - q_{1-2}, \quad T_2 > T_1. \tag{9}$$

The heat flux at the interface was computed for a range of temperature reservoirs for each of the interfaces studied here. Figure 10 indicates that the heat flux is linear with temperature difference. Our analysis also shows that the magnitude of the temperature is immaterial. Although we get no rectification at 0 K (as expected), this case was added to ensure that the rectification was not an artifact of the way we performed the simulation.

The linear dependence in temperature is not unexpected in a device that is confined such as a wire. In the present simulations, a periodic solid was considered. However, if the dimension of the periodic solid is small, the phonons in the periodic direction will still be confined in those periodic directions. Because the computed heat flux is linear in ΔT, we can estimate the slope to obtain a constant thermal conductance for each interface. The temperature differences of 0 K, 30 K, 60 K, 90 K, 120 K, 150 K, 180 K, 210 K, 240 K, 270 K, and 300 K correspond to cold bath temperatures of 10 K, 20 K, 40 K, 60 K, 80 K, 100 K, 120 K, 140 K, 160 K, 180 K, and 200 K, respectively. Figure 11 shows how thermal rectification is manifested in each interface by comparing the magnitude of the forward and reverse directions. In the perfect interface the transport is favored in the direction of the krypton to the argon. In the diffuse interface labeled fine, it appears that there is no noticeable directional dependence. In the diffuse interface label coarse the result is the opposite of the perfect interface case giving a preferred transport direction of the argon to the krypton. This transition in the preferred direction of transport is a result of inelastic scattering at the interface. In the perfect interface the high frequency modes in argon are not able to contribute to the thermal transport since they are not allowed to transmit in to the krypton while all of the modes in the krypton are allowed to transmit at least partially into the argon. When we look at the diffuse interfaces we begin to see some probability of transmission of the higher frequency modes in argon into the krypton therefore opening up additional modes to contribute to the thermal transport in the argon to krypton direction, but no additional modes in the krypton to argon direction. As the level of diffusion or the size of the diffusion region is increased we see increased levels of inelastic scattering at the interface which again allows for a greater percentage of higher frequency modes in argon to contribute to the thermal transport. If we were to increase the region of diffusion we would eventually reach the case where all phonons that interacted with the interface are inelastically scattered and no rectification would result.

IV. CONCLUSION

Theoretical studies of thermal rectification have been performed, but this work looks specifically at frequency dependence of phonon transmission at an interface in both directions. The AMM and DMM do not contain any directional dependence on the transmission coefficient, therefore, we are not able to compare the value we calculated to the theoretical prediction of these models unless we assume an average transmission coefficient. Clearly from the wave-packet results here, there is a difference in phonon transmission from the argon to the krypton than from the krypton to the argon even when low levels of inelastic scattering occur at the interface. With a strong frequency dependence in phonon transmission at perfect and diffuse interfaces thermally rectifying materials are possible to obtain when little inelastic scattering occurs. As the interface is degraded transport appears to shift from a preferred direction of krypton to argon to the argon to krypton.

ACKNOWLEDGMENTS

Special thanks to Dr. Ying Sun and Zhiting Tian at Drexel University for their useful conversations.

[1]H. Kageshima and A. Fujiwara, Appl. Phys. Lett. **96**, 193102 (2010).
[2]T. Xu, Z. Wang, J. Miao, X. Chen, and C. M. Tan, Appl. Phys. Lett. **91**, 042108 (2007).
[3]X. Zhou, K. Uchida, and S. Oda, Appl. Phys. Lett. **96**, 092112 (2010).
[4]W. Kim, J. Zide, A. Gossard, D. Klenov, S. Stemmer, A. Shakouri, and A. Majumdar, Phys. Rev. Lett. **96**, 045901 (2006).
[5]C. Starr, Physics **7**, 15 (1936).
[6]M. Terraneo, M. Peyrard, and G. Casati, Phys. Rev. Lett. **88**, 094302 (2002).
[7]B. Li, L. Wang, and G. Casati, Phys. Rev. Lett. **93**, 184301 (2004).
[8]B. Hu and L. Yang, Chaos **15**, 015119 (2005).
[9]D. Segal and A. Nitzan, J. Chem. Phys. **122**, 194704 (2005).
[10]D. G. Walker, Proceedings of the Joint ASME-ISHMT Heat Transfer Conference, IIT Guwahati, India, 4–6 January 2006 (ASME, New York, 2006).
[11]G. Wu and B. Li, Phys. Rev. B **76**, 085424 (2007).
[12]N. A. Roberts and D. G. Walker, Proceedings of ITherm 2008, Walt Disney World Resort Orlando, FL, USA, 28–30 May 2008 (IEEE, New York, 2008).
[13]J. Miller, W. Jang, and C. Dames, Proceedings of 3rd Energy Nanotechnology International Conference, Jacksonville, FL, 10–14 August 2008 (ASME, New York, 2008).
[14]M. Alaghemandi, E. Algaer, M. Bohm, and F. Muller-Plathe, Nanotechnology **20**, 115704 (2009).
[15]C. W. Chang, D. Okawa, A. Majumdar, and A. Zettl, Science **314**, 1121 (2006).
[16]M. Hu, P. Keblinski, and B. Li, Appl. Phys. Lett. **92**, 211908 (2008).
[17]N. A. Roberts and D. G. Walker, "Molecular dynamics simulation of thermal rectification in Ar/Kr interfaces," J. Heat Transfer (to be published).
[18]E. T. Swartz and R. O. Pohl, Rev. Mod. Phys. **61**, 605 (1989).
[19]P. K. Schelling, S. R. Phillpot, and P. Keblinski, Appl. Phys. Lett. **80**, 2484 (2002).
[20]P. K. Schelling, S. R. Phillpot, and P. Keblinski, J. Appl. Phys. **95**, 6082

(2004).
[21]L. Sun and J. Y. Murthy, Proceedings of ITherm, Orlando, Florida, 28–30 May 2008 (IEEE, New York, 2008), pp. 1078–1086.
[22]Z. Tian, B. White, and Y. Sun, Appl. Phys. Lett. **96**, 263113 (2010).
[23]S. Plimpton, "LAMMPS-large-scale atomic/molecular massively parallel simulator," http://lammps.sandia.gov/
[24]Y. F. Chen, D. Y. Li, J. K. Yang, Y. H. Yu, J. R. Lukes, and A. Majumdar, Physica B **349**, 270 (2004).
[25]J. Behari and B. B. Tripathi, Lett. Nuovo Cimento **3**, 381 (1970).
[26]H. R. Glyde and M. G. Smoes, Phys. Rev. B **22**, 6391 (1980).
[27]W. B. Daniels, G. Shirane, B. C. Frazer, H. Umebayashi, and J. A. Leake, Phys. Rev. Lett. **18**, 548 (1967).
[28]H. Zhao and J. B. Freund, J. Appl. Phys. **105**, 013515 (2009).
[29]Z. M. Zhang, *Micro/Nanoscale Heat Transfer* (McGraw-Hill, New York, 2007).